



A Study on Wear Behaviour of Electrical Discharge-Coated Magnesium Alloy

U. Elaiyaran¹ · V. Satheeshkumar¹ · C. Senthilkumar¹

Received: 24 November 2018 / Revised: 4 January 2019 / Accepted: 13 January 2019 / Published online: 23 January 2019
© Springer Nature Switzerland AG 2019

Abstract

Wear behaviour of ZE41A magnesium alloy coated with WC/Cu using electrical discharge coating (EDC) has been investigated in this study. The wear test was conducted with pin-on-disc machine using different conditions such as normal load of 1.5 kg, 2.5 kg, 3.5 kg and sliding speed of 100 rpm, 200 rpm, 300 rpm and sliding time of 3 min, 5 min, 7 min through L9 Taguchi orthogonal array to study the effect of sliding parameters on the wear characteristics. A wear transition map was constructed to describe the different wear conditions such as mild wear, severe wear and ultra severe wear. The main wear mechanisms for each wear regime were identified and classified through wear mechanism map. The worn-out specimens were characterized using scanning electron microscope (SEM) to identify the various wear mechanisms.

Keywords ZE41A magnesium alloy · Electrical discharge coating · Wear mechanism map · Mild wear

1 Introduction

Lightweight material is an important role in engineering application to reduce the weight of the component particularly in the field of automobile and aerospace. Among the lightweight materials, magnesium alloy is the lightest metallic material and it has superior properties such as low density, good specific strength and good castability [1, 2]. Moreover, it has good impact resistance, damping capacity, electrical and thermal conductivity to make component in the suitable structural application. Despite attractive ranges of properties, magnesium alloys have lower mechanical properties and poor corrosion as well as wear resistance than other light materials [3–5]. Mainly wear and corrosion are take place on the component of surface due to poor environmental condition. To overcome the above said problems, several coating processes, such as physical vapour deposition (PVD) and chemical vapour deposition (CVD), have been used to improve the wear resistance. Since they incurred higher costs, a well-recognized and economic method of electrical discharge coating (EDC) has been developed. It is the process of coating method to improve the surface

properties of the materials with existing electrical discharge machining (EDM). There have been many reports on magnesium alloy coated with various coating processes; however, the wear behaviour of such coatings is not well understood.

Staia et al. [6] have investigated the friction and wear behaviour of Ni–P coating on AISI 1020 plain carbon steel using pin-on-disc configuration with counterface disc of AISI 52,100 steel. Mainly sliding distance has been chosen as sliding parameter with range of 130, 520 and 1040 m. It is concluded that the wear rate and coefficient of friction (COF) increases with increase in the sliding distance. In this wear resistance of Ni–P coating, severe wear is mostly dominating the sliding parameters. Chen and Wang [7] have improved the wear resistance of electrolyzed nickel coated with TiC reinforced nickel aluminide matrix composite. It can be found that the intermetallic composite coating gives tremendous wear resistance under both room- and high-temperature sliding wear conditions. Lasa and Rodriguez [8] studied the wear behaviour of Al–Si alloys with addition of Cu and Ni using pin-on-disc method. It is concluded from the result of their study that the coefficient of wear of alloy is dependent on the disc speed under constant load and sliding distance conditions. At higher speed, the wear mechanism was identified to be of oxidative nature, low sliding speed accelerated transition to adhesive wear, and the rate of wear was increased dramatically. Palaniappa and Seshadri [9] investigated the wear and friction characteristics of electro-deposited Ni/W alloy under

✉ U. Elaiyaran
elaiyaran555@gmail.com

¹ Department of Manufacturing Engineering, Annamalai University, Chidambaram, Tamilnadu 608002, India

different sliding conditions. The wear test was conducted in low load and low sliding velocity against hardened steel counterface. It was confirmed that the oxidative and adhesive wear mechanisms were found in lower sliding condition and also reported that W in the Ni/W alloy led to the formation of constant and protective transfer layer on the steel counter body. Alirezaei et al. [10] improved the wear behaviour of Ni–P and Ni–P–Al₂O₃ electroless coatings with AISI 1045 steel discs under sliding distance of 200, 400, 600 in metres. It was found that the wear loss increases with increases in sliding distance and abrasive wear is the most dominant wear mechanism in this coating. Krishnaveni et al. [11] studied the wear resistance of electroless Ni–B coating under normal load of 20, 30 and 40 N and constant sliding speed of 0.5 m/s using pin-on-disc tribosystem. It is found that as the normal load increases from 20 to 40 N, specific wear rate increases. It has been observed from the SEM image that the wear track pattern reveals bright and fine surface with fine grooves along the sliding direction. The wear mechanism of adhesive was found in the electroless Ni–B coatings.

Kaviti et al. [12] investigated the effect of dry sliding wear behaviour of boron nitride reinforcement (0.5%, 1.5% and 2.5%) on pure magnesium. Sliding condition of normal load is 5 N, 7 N and 10 N and sliding speed of 0.6, 0.9 and 1.2 m/s against steel disc at room temperature conditions on the response of wear rate and friction coefficient. From the experimental results, the wear rate increases at all levels of sliding speed and friction coefficient increased at all levels of normal load. Mainly three wear mechanisms occurred on the surface, namely groove or abrasion at 5 N, oxidation and delamination at 10 N. Hu et al. [13] improved the wear behaviour of wrought AZ31 magnesium alloy specimens prepared by direct extrusion and extrusion shear method. The responses of such wear rate and coefficient of friction have been evaluated under different sliding loads and frequencies in dry sliding pin-on-disc setup. From the evaluation, it was observed that when there are increases in loads and frequencies, the wear mechanism changes from mild wear (adhesion, abrasion and oxidation) to severe wear (delamination, plastic deformation and melting). El-Morsy [14] examined the wear study of AZ61-extruded magnesium alloy during dry sliding conditions. The experiments were conducted using a pin-on-ring-type apparatus against a stainless steel counterface. It was observed that the sliding wear behaviour can be classified in to two wear regimes, mild wear regime and severe wear regime. García et al. [15] investigated wear behaviour of AZ91 magnesium alloy reinforcement of 5 and 10 vol.% SiC particles under sliding parameters of load (10–250 N) and sliding speed (0.1,

0.3, 0.5 and 1 m/s) against 1045 steel disc counterface body by pin-on-disc apparatus. At higher sliding parameters (0.5–1 m/s and 150–250 N), melt mechanism occurred due to higher frictional heat that increases the surface melting, and it was also found the presence of silicon carbide does not improve the wear resistance of mechanism alloy.

From the past literature, several researchers focused on the wear behaviour of magnesium alloy using various techniques such as PVD, CVD, electroless plating and other coating techniques, but to the best of our knowledge no research was found on the wear behaviour of magnesium alloy using EDC. Hence, in the present research, ZE41A magnesium alloy has been coated with tungsten carbide–copper (WC/Cu) powder metallurgy (P/M) electrode using EDC. Hence, the wear behaviour of WC/Cu-coated magnesium alloy was investigated. Further wear transition and wear mechanism maps were drawn to find out the various wear regimes. Different wear mechanisms were found from the worn-out specimen through scanning electron microscope (SEM), and energy dispersive spectroscopy (EDS) analysis has been carried out to find the various elements deposited on the coated surface of the work piece.

2 Experimental Details

2.1 Electrode Preparation and Coating

In the present study, ZE41A magnesium alloy has been utilized as workpiece material and its chemical composition is given in Table 1. The tungsten carbide (WC) and copper (Cu) powder particles of 4 µm were chosen as electrode material because of high strength and good electrical conductivity. The powders were mixed in the ratio of 70:30 (wt%) proportion and compacted using punch-and-die setup with diameter of 10 mm under various compaction loads. Subsequently the compacted electrode was sintered in the tubular furnace under argon atmosphere, about 600 °C for 20 min. Further the sintered electrodes were cooled in the furnace. The experiment was conducted with prepared electrode with EDM oil as dielectric fluid using conventional die sinking EDM machine. The prepared electrode was polished and buffed to make it flat prior to experimentation. The experiments had been carried out using constant voltage of 40 V, inter electrode gap of 0.5 mm, compaction load of 150 MPa, current of 4 A and pulse time of 90 µs with fixed time interval of 10 min.

Table 1 Chemical composition of ZE41A magnesium alloy

Si	Cu	Zn	Zr	Fe	TRE	Ni	Mn	Al	Mg
0.003	0.002	3.80	0.60	0.004	1.18	0.002	0.003	0.006	Bal

2.2 Wear Test

The wear tests were carried out on a pin-on-disc tribotester (TR-20-PHM-M1, Ducom, India) as shown in Fig. 1. The wear samples have been prepared with the dimension of 10 mm diameter and 20 mm length is shown in Fig. 2a. The counterface disc was made of EN31 steel material with 50 mm diameter as shown in Fig. 2b. The hardness of the counterface disc was 65HR_C and it was polished well with abrasive emery sheet of 1000 grade. The wear tests were conducted with three different sliding parameter conditions such as normal load (1.5 kg, 2.5 kg, 3.5 kg), sliding speed (100 rpm, 200 rpm, 300 rpm), sliding time (3 min, 5 min, 7 min) and track diameter of 20 mm. After each test was conducted, the specimens were cleaned to ensure the accuracy of measurement. The weight loss of the worn specimen was noted. The specific wear rate of experiments was calculated by the given formula:

$$W_s = \Delta m / \rho \cdot t \cdot F_N \cdot V_s \text{ (mm}^3\text{/Nm)},$$

where Δm is the mass losses of the pin samples (g), ρ is the density of the test sample (g/mm³), t is the sliding time (s), V_s is the sliding speed (m/s), and F_N is the normal load (N).

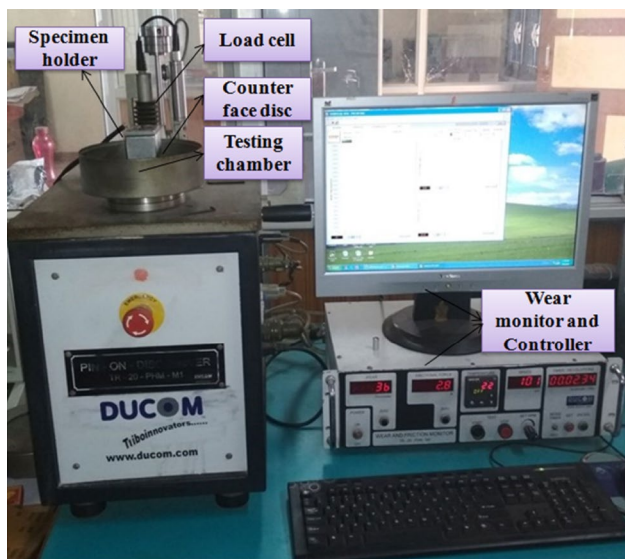


Fig. 1 Pin-on-disc apparatus (TR-20-PHM-M1)

Fig. 2 a Wear specimens and b counterface disc (EN31 steel)



2.3 Experimental Design

The experiment was carried out to analyse the effect of Sliding parameters on wear rate and coefficient of friction of ZE41A magnesium alloy coated with WC/Cu composite. For the present investigation, standard Taguchi L9 (3³) orthogonal array was chosen. The control parameters and their levels are given in Table 2. Table 3 shows the orthogonal array and associated experimental results for wear rate (WR) and coefficient of friction (COF).

3 Result and Discussion

3.1 Microstructure of WC/Cu Coatings

Figure 3a shows WC/Cu coated on the ZE41A magnesium alloy during EDC with low compaction load (150 MPa), high current (4 A) and pulse time (90 μ s). Figure 3b reveals that the various elements deposited on the coated surface confirm the deposition of the materials. The quantities of electrode materials Cu and W were 0.50 and 0.39, respectively.

3.2 Effect of Process Parameters on Wear Rate

The mean effect of the wear rate was plotted against the normal loads, sliding speed and sliding time as shown in Fig. 4. From Fig. 4a, wear rate increases linearly with increase in normal load, because increases in contact pressure and local temperature at contact surface of the materials result in higher wear rate, which leads to the removal of the coated material. A similar investigation was reported in a study on wear of Al-SiC composites [16].

Table 2 Control factors and their levels

Control factors	Unit	Level		
		I	II	III
Normal load	kg	1.5	2.5	3.5
Sliding speed	rpm	100	200	300
Sliding time	min	3	5	7

Table 3 Experimental result using L9 orthogonal array

Ex. no.	Control factors			Wear properties	
	Normal load (kg)	Sliding speed (rpm)	Sliding time (min)	Wear rate (mm ³ /Nm)	Coefficient of friction
1	1.5	100	3	0.0001819	0.0150166
2	1.5	200	5	0.0002355	0.0194853
3	1.5	300	7	0.0002598	0.0254347
4	2.5	100	5	0.0002295	0.0199473
5	2.5	200	7	0.0002896	0.0280291
6	2.5	300	3	0.0002556	0.0274187
7	3.5	100	7	0.0002725	0.0298055
8	3.5	200	3	0.0002892	0.0261874
9	3.5	300	5	0.0003336	0.0382568

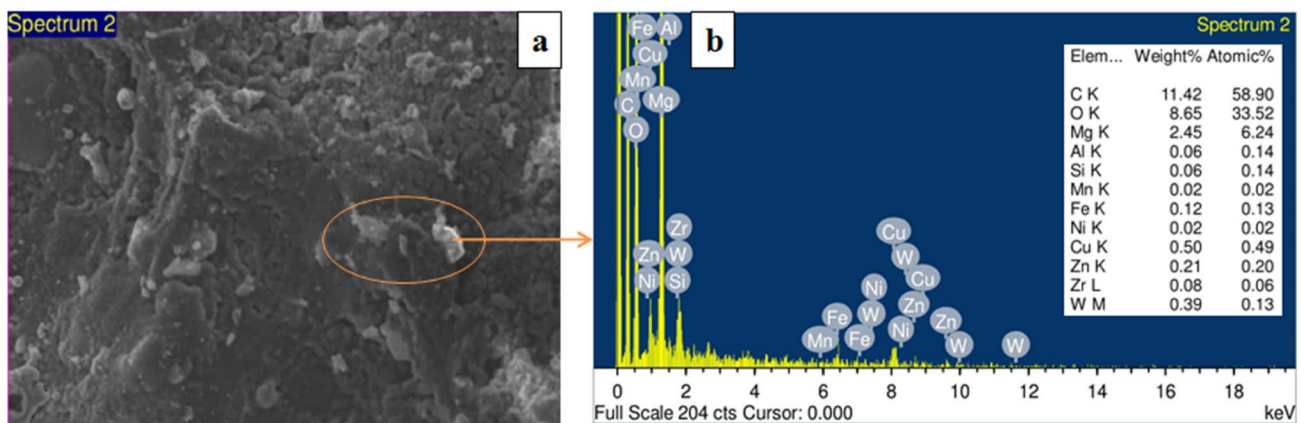
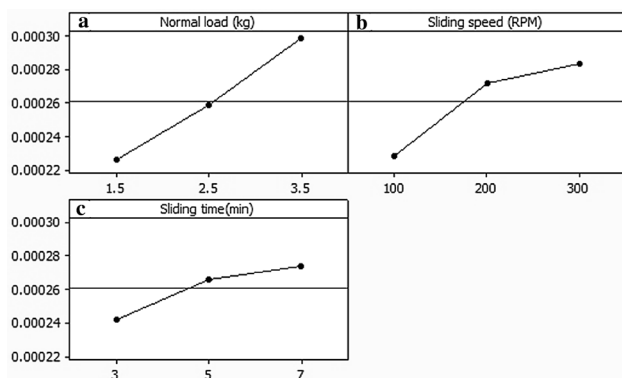
**Fig. 3** a SEM image for WC/Cu coating at 150 MPa, 4 A and 90 μ s and b EDS peak plot for WC/Cu coating**Fig. 4** Mean effect plot for wear rate: a normal load, b sliding speed and c sliding time

Figure 4b reveals that wear rate increases with the increasing sliding speed up to 200 rpm and any further increase in sliding speed makes the wear rate increase slightly. This may be due to continuous friction between both contact surfaces, which resulted in the removal of coating material

from the surface with the formation of cracks resulted in delamination.

Sliding time is one of the important parameters of the wear rate. In Fig. 4c, wear rate slightly increases with the increment of sliding time. As the duration of sliding increases, the higher temperature generated over longer time between the disc and pin increases the frictional heat, resulting in melting of coated surface.

3.3 Effect of Process Parameters on Coefficient of Friction

Figure 5 shows the mean effect plot for coefficient of friction against normal load, sliding speed and sliding time. In this plot, coefficient of friction increases with increases in normal load, sliding speed and sliding time. Figure 5a exhibits the normal load versus coefficient of friction. Coefficient of friction (COF) increases with normal load linearly, and due to higher applied loads, the coated material impedes the movement of disc and pin [17]. It is cleared from Fig. 5b, as sliding speed increases,

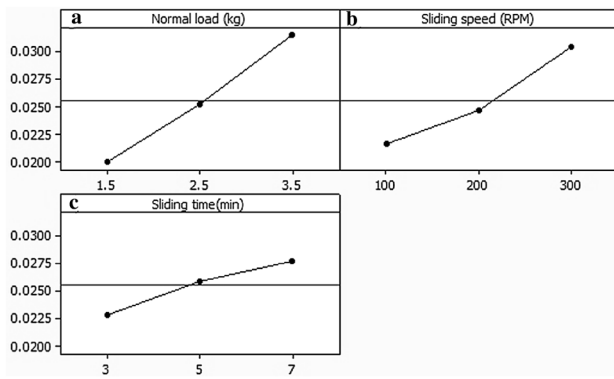


Fig. 5 Mean effect plot for coefficient of friction: **a** normal load, **b** sliding speed and **c** sliding time

coefficient of friction increases. This could be because temperature shoots up significantly and temperature gradient increases. This leads to higher heat dissipation, and flow ability of the material results in the occurrence of smearing and scratches on the surface. Friction coefficient increases with increases in sliding time as shown in Fig. 5c. Because of higher sliding time, the material is worn out into irregular shaped micron size debris, which is entrapped into the wear track and leads to increase in COF.

3.4 Wear Rate Map

Wear rate maps are essential to understand the wear characteristics of desired material on range of different sliding conditions. Wear rate map is the graphical illustration to study the effect of sliding parameters such as normal load and sliding speed on wear rate, and the curves of the wear rate have been drawn as contours. The adjustment in the direction of the contour lines represents the mode of wear (mild wear, severe wear and ultra severe wear). The contour wear rate maps have been constructed using Minitab software and wear rate data by considering normal load on X-axis and sliding speed on Y-axis, which resulted in the wear rate on Z-axis. Every contour line represents the wear rate for different normal load and sliding speed conditions [18]. Figure 6 shows the wear rate map and wear transition map of ZE41A magnesium alloy coated with WC/Cu with normal load and sliding speed conditions. From wear rate map, it is cleared that the horizontal contour lines indicate the effect of parameter on vertical axis and vertical contours indicates the effect of parameter on horizontal axis. The wear rate of WC/Cu-coated magnesium alloy is minimum in the condition of lower normal and sliding speed. Conversely it is maximum at higher applied load and sliding speed conditions.

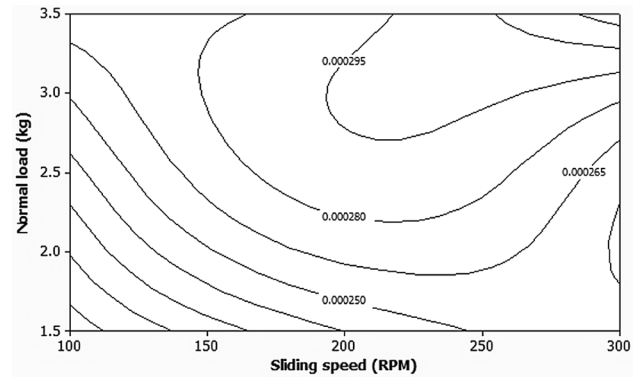


Fig. 6 Wear rate map for WC/Cu-coated Mg alloy

3.5 Wear Transition Map

The sudden peak of the wear rates has been indicated by change in direction of contour lines. Hence, the wear rate map is easy-to-build wear map which is called wear regime map or wear transition map. The constructed wear transition map provides the context to study about different wear mechanisms in each region under different dry sliding parametric conditions. Boundary surface of predominant wear and their transitions is important for constructing the wear transition map. The wear transition map describes the minimum number of wear mechanisms in the given operating conditions. By investigating the wear contour maps, it is observed that equal line spacing and lack of curvature typically indicate the same dominant mechanism. Valley and plateaus indicated some changes in the wear mode. In this method, different wear mechanisms can be identified in the worn surface regions [18]. Figure 7 shows the wear transition map for ZE41A magnesium alloy. It illustrates three different wear regimes, namely mild wear, severe wear and ultra severe wear. The transition boundary surfaces were formed between mild wear to severe wear and severe to ultra severe wear [19].

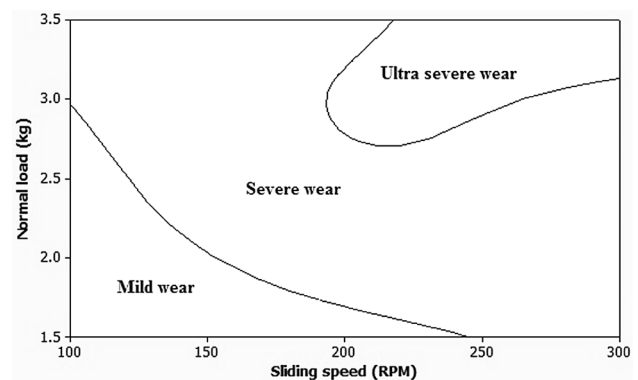


Fig. 7 Wear transition map for WC/Cu-coated Mg alloy

3.6 Wear Mechanism Map

The wear mechanism map of the ZE41A magnesium alloy coated with WC/Cu was developed from the combination of the calculated wear rate against parameters of normal load and sliding speed. The wear mechanism map identifies the regions with the predominating mechanisms accompanied by SEM microstructure. Wear mechanism map of ZE41A magnesium alloy coated with WC/Cu against EN31 steel counterface disc is shown in Fig. 8. Wear mechanism map was developed to summarize the data and models for wear, showing how the mechanisms interface. This surface area or region has been separated by transition contour lines. Wear mechanism map was constructed to investigate this pattern of wear behaviour. Zhang and Alpas [20] have recommended that wear mechanism map is a practical tool to evaluate the wear performance conditions using tribosystem and serves as the guideline to select the appropriate wear-resistant materials and suitable counter faces. In the wear mechanism map, three wear regimes have been developed, namely

mild wear, severe wear and ultra severe wear. In real application purpose, this wear regime can be regarded as the “safe” because the wear rate value is typically low under the steady-state condition.

The ploughing or grooves were observed at low normal load of 1.5 kg and sliding speed of 100 rpm due to the effect of movement of hard particles relative to the contact surface parallel to the sliding direction [21]. The depth of the grooves depends on the hardness of the particles. The worn-out surface shown in Fig. 9 has mostly grooves, indicative of abrasion being dominant wear mechanism. In this condition, the WC is pulled out from the coated surface because the wear of the Cu is more rapid.

Oxidation wear occurs at normal applied load of 1.5 kg and the sliding speed of 200 rpm. Due to continued sliding between the two surfaces, sufficient amount of temperature is generated between the contact surfaces which resulted in oxidation wear, as depicted in Fig. 10 [22]. Lim [23] concluded that the low sliding velocity does not generate the sufficient flash temperature to form oxidation on the surface, which is the dominant wear mechanism.

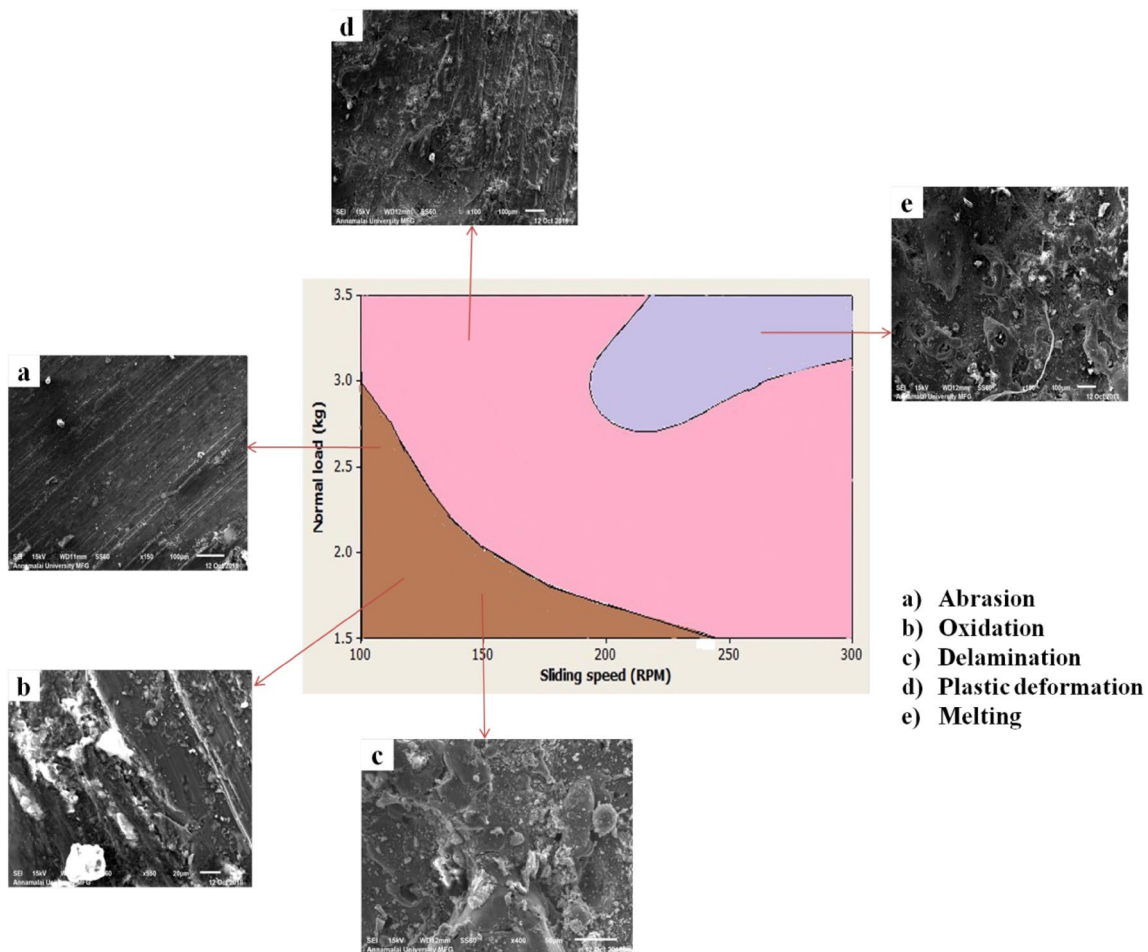


Fig. 8 Wear mechanism map of ZE41A magnesium alloy coated with WC/Cu against EN31 steel counterface

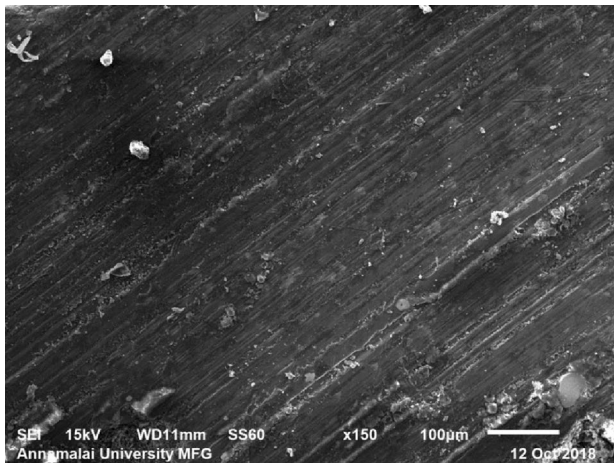


Fig. 9 SEM micrograph of abrasion at 1.5 kg and 100 rpm

Under more severe contact with normal load and sliding speed of 1.5 kg and 300 rpm, cracks are introduced on either side of the wear track. These are perpendicular to sliding way leading to increment of subsurface crack. This resulted in detachment of coated material with flake- or sheet-like particles in the form of delamination as depicted in Fig. 11. The similar finding was observed by Sharma et al. [24] that the high sliding speed regardless of the normal load results in surface cracks due to the presence of hard particles between the contact surfaces during constant rotation of pin surface, which influence the wear mechanism.

When the normal load and sliding speed increased beyond 2.5 kg and 200 rpm, the oxide formation on the coated surfaces has been increased. The formed oxide patches plastically deformed on the sliding surfaces which evident from Fig. 12. It was concluded that the oxide layer formed is thicker and more continuous under such conditions and was almost hotter and more plastic deformed [25].

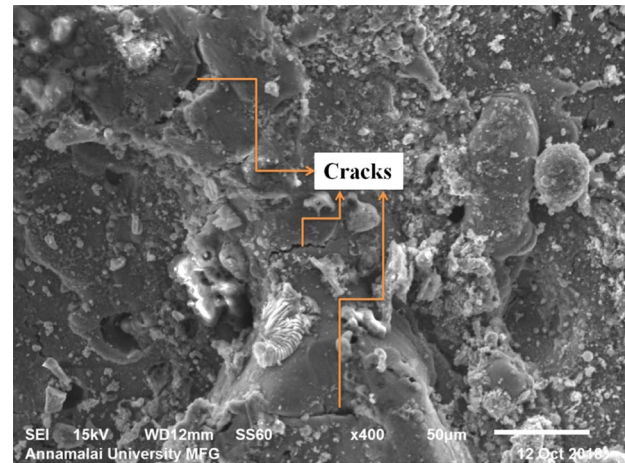


Fig. 11 SEM micrograph of delamination at 1.5 kg and 300 rpm

It was concluded that high normal load and sliding speed generate high temperature leading to plastic deformation. This attributed that it would reduce the yield strength of the coated surface, as a plastically deformed layer spread out on the coated surface along the sliding direction.

Melting was observed in the higher sliding condition of normal load 3.5 kg and sliding speed of 300 rpm. Under this condition, high temperature was generated, due to friction between the contact surfaces. Temperature generated on the surface was high enough to melt the coating surface, owing to thermal gradient, and resulted in WC pullout from the surface. This indicates that the wear mechanism is ultra severe as shown in Fig. 13. It was clarified by Chen and Alpas [19] that the highest applied load and sliding speed increase the local temperature between the disc and pin surface. Continued sliding speed raises the flash temperature between contact surfaces resulting in the formation of melting [26].

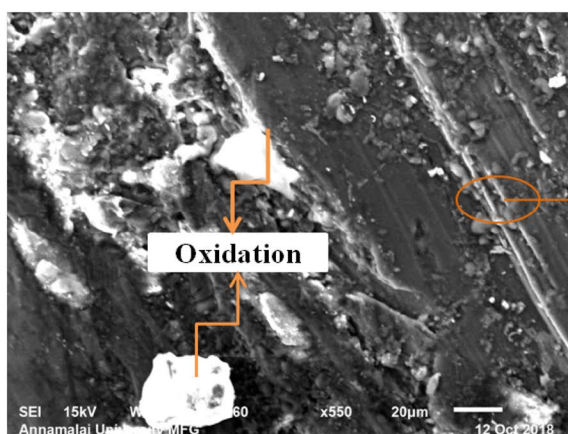
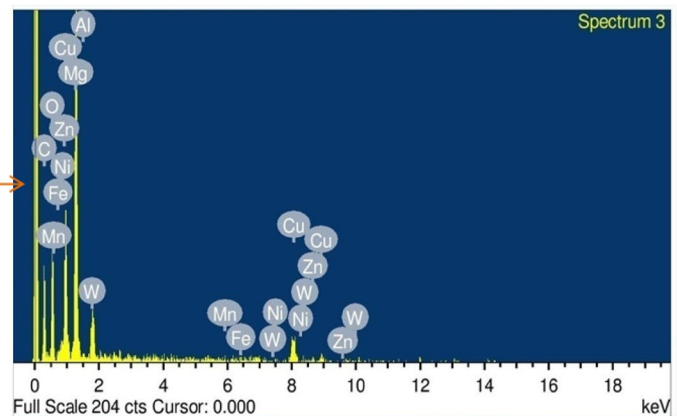


Fig. 10 SEM micrograph of oxidation at 1.5 kg and 200 rpm



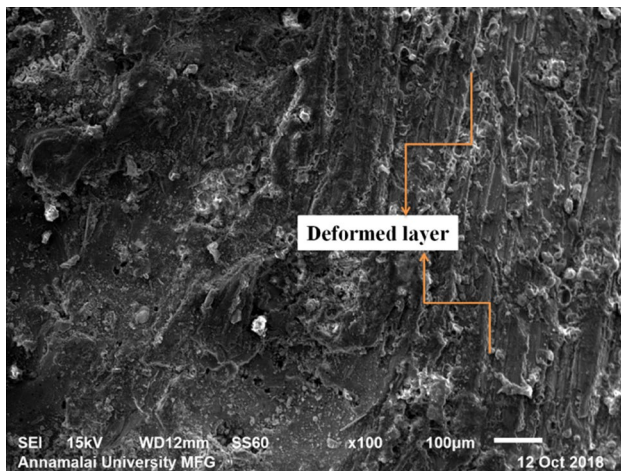


Fig. 12 SEM micrograph of plastic deformation at 2.5 kg and 200 rpm

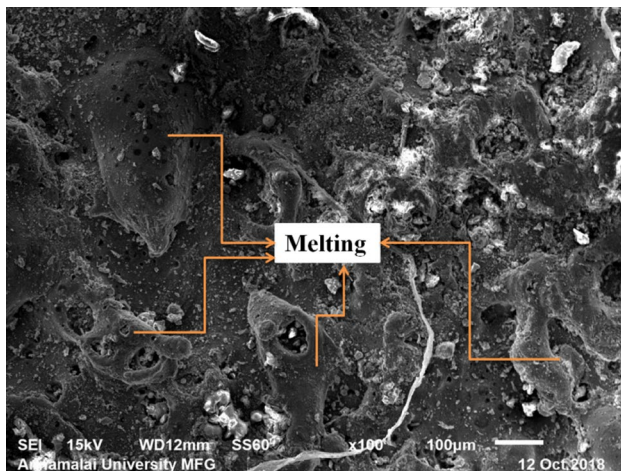


Fig. 13 SEM micrograph of melting at 3.5 kg and 300 rpm

4 Conclusion

The wear behaviour of ZE41A magnesium alloy coated with WC/Cu has been studied using different sliding conditions of normal load, sliding speed and sliding time on the responses of wear rate and coefficient of friction. It was concluded that the wear rate and coefficient of friction increases with increase of normal load, sliding speed and sliding time. Wear rate map and wear transition map were constructed to study the effect of the sliding condition. Wear mechanism map was developed to identify the wear regime of mechanism, namely mild wear, severe wear and ultra severe wear. Surface morphology of worn surface was evaluated using SEM. The influences of wear mechanisms of abrasion, oxidation, delamination, plastic

deformation and melting were identified and summarized in the wear mechanism map. From the wear mechanism map, abrasion (1.5 kg and 100 rpm), oxidation (1.5 kg and 200 rpm) and delamination (1.5 kg and 300 rpm) occurred in the mild wear regime. Plastic deformation (2.5 kg and 200 rpm) was observed in severe wear regime and melting (3.5 kg and 300 rpm) was formed in ultra severe wear regime.

Acknowledgements The authors wish to offer their heartfelt thanks to the University Grant Commission (UGC), New Delhi for awarding fellowship for doing research through the Award Letter No: F1-17.1/2017-18/RGNF-2017-18-SC-TAM-34647/(SA-III/Website) dated 27/07/2017 (A study on electro-discharge machining of ZE41A magnesium alloy). The authors are also grateful to the Centre for Materials Joining and Research (CEMAJOR), Department of Manufacturing Engineering, Annamalai University for providing lab facilities to conduct the experiments.

Compliance with Ethical Standards

Conflict of interest There is no conflict of interest.

References

1. Prakash DL, Prasanna B, Regener D (2005) Computational microstructure analyzing technique for quantitative characterization of shrinkage and gas pores in pressure die cast AZ91 magnesium alloys. *Comput Mater Sci* 32(3–4):480–488
2. Wang RM, Eliezer A, Gutman EM (2003) An investigation on the microstructure of an AM50 magnesium alloy. *Mater Sci Eng A* 355(1–2):201–207
3. Mehta DS, Masood SH, Song WQ (2004) Investigation of wear properties of magnesium and aluminum alloys for automotive applications. *J Mater Proc Technol* 155:1526–1531
4. Mordike BL, Ebert T (2001) Magnesium: properties-applications-potential. *Mater Sci Eng A* 302(1):37–45
5. Rauber C, Lohmüller A, Opel S, Singer RF (2011) Microstructure and mechanical properties of SiC particle reinforced magnesium composites processed by injection molding. *Mater Sci Eng A* 528(19–20):6313–6323
6. Staia MH, Castillo EJ, Puchi ES, Lewis B, Hintermann HE (1996) Wear performance and mechanism of electroless Ni/P coating. *Surf coat Technol* 86:598–602
7. Chen Y, Wang HM (2004) Microstructure and wear resistance of a laser clad TiC reinforced nickel aluminides matrix composite coating. *Mater Sci Eng A* 368(1–2):80–87
8. Lasa L, Rodriguez-Ibabe JM (2002) Effect of composition and processing route on the wear behaviour of Al–Si alloys. *Scri Mater* 46(6):477–481
9. Palaniappa M, Seshadri SK (2008) Friction and wear behavior of electroless Ni–P and Ni–W–P alloy coatings. *Wear* 265(5–6):735–740
10. Alirezai S, Monirvaghefi SM, Salehi M, Saatchi A (2007) Wear behavior of Ni–P and Ni–P–Al₂O₃ electroless coatings. *Wear* 262(7–8):978–985
11. Krishnaveni K, Narayanan TS, Seshadri SK (2005) Electroless Ni–B coatings: preparation and evaluation of hardness and wear resistance. *Surf Coat Technol* 190(1):115–121

12. Kaviti RVP, Jeyasimman D, Parande G, Gupta M, Narayanasamy R (2018) Investigation on dry sliding wear behavior of Mg/BN nanocomposites. *J Mag Alloys* 6(3):263–276
13. Hu HJ, Sun Z, Ou ZW, Wang XQ (2017) Wear behaviors and wear mechanisms of wrought magnesium alloy AZ31 fabricated by extrusion-shear. *Eng Fail Analy* 72:25–33
14. El-Morsy AW (2008) Dry sliding wear behavior of hot deformed magnesium AZ61 alloy as influenced by the sliding conditions. *Mater Sci Eng A* 473(1–2):330–335
15. García-Rodríguez S, Torres B, Maroto A, López AJ, Otero E, Rams J (2017) Dry sliding wear behavior of globular AZ91 magnesium alloy and AZ91/SiC_p composites. *Wear* 390:1–10
16. Gul F, Acilar M (2004) Effect of the reinforcement volume fraction on the dry sliding wear behaviour of Al–10Si/SiC_p composites produced by vacuum infiltration technique. *Comp Sci Tech* 64(13–14):1959–1970
17. Schwartz CJ, Bahadur S (2001) The role of filler deformability, filler–polymer bonding, and counterface material on the tribological behavior of polyphenylene sulfide (PPS). *Wear* 251(1–12):1532–1540
18. Wilson S, Alpas AT (1997) Wear mechanism maps for metal matrix composites. *Wear* 212(1):41–49
19. Chen H, Alpas AT (2000) Sliding wear map for the magnesium alloy Mg–9Al–0.9Zn (AZ91). *Wear* 246(1–2):106–116
20. Zhang J, Alpas AT (1997) Transition between mild and severe wear in aluminium alloys. *Acta Mater* 45(2):513–528
21. Mondal AK, Rao BC, Kumar S (2007) Wear behaviour of AE42 + 20% saffil Mg-MMC. *Tribo Int* 40(2):290–296
22. Liu Y, Asthana R, Rohatgi P (1991) A map for wear mechanisms in aluminium alloys. *J Mater Sci* 26(1):99–102
23. Lim SC (2002) The relevance of wear-mechanism maps to mild-oxidational wear. *Tribo Int* 35(11):717–723
24. Sharma SC, Anand B, Krishna M (2000) Evaluation of sliding wear behaviour of feldspar particle-reinforced magnesium alloy composites. *Wear* 241(1):33–40
25. Venkataraman B, Sundararajan G (1996) The sliding wear behaviour of Al/SiC particulate composites-I. Macrobehaviour *Acta Mater* 44(2):451–460
26. Lim CYH, Lim SC, Gupta M (2003) Wear behaviour of SiC_p-reinforced magnesium matrix composites. *Wear* 255(1–6):629–637